Hindawi
Structural Control and Health Monitoring
Volume 2024, Article ID 6645626, 19 pages
https://doi.org/10.1155/2024/6645626

Research Article

LSTM-Based Approach for Stable Identification of Modal Damping Ratio in Building Structures

Da Yo Yun, Byung Kwan Oh, Kanghyun Park, and Hyo Seon Park

Department of Architecture and Architectural Engineering, Yonsei University, Seoul 120-749, Republic of Korea

Correspondence should be addressed to Hyo Seon Park; hspark@yonsei.ac.kr

Received 15 June 2023; Revised 27 September 2023; Accepted 18 December 2023; Published 2 January 2024

Academic Editor: Yongchao Yang

Modal parameters are used as safety assessment indicators for evaluating the structural integrity of buildings in various ways. In particular, the modal damping ratio plays a crucial role in accurately predicting the serviceability and safety of buildings, starting from the initial design stage. However, the identification results of the modal damping ratio can become unstable due to measurement time, initial configuration conditions used in the analysis, and nonstationary responses included in the structural response. To address the instability issue, this study proposes a long short-term memory-based frequency domain decomposition (FDD-LSTM) method. The FDD-LSTM method utilizes the acceleration response of the building as input data and the modal damping ratio obtained from the FDD method as output data, constructing an LSTM network model for the relationship between the acceleration response and modal damping ratio. The FDD-LSTM method exhibited a discrepancy of less than 0.02% compared to the reference value of the modal damping ratio obtained through free vibration response. Furthermore, when applied to data acquired from an actual building, the method demonstrated a variance of approximately 5%. The proposed FDD-LSTM method is validated for stability performance using a three-degree-of-freedom numerical analysis model, a 3-story steel frame structure model, and a 117-story high-rise building. The FDD-LSTM method, trained on a large dataset, enables generalized estimation and addresses instability issues related to modal damping ratio.

1. Introduction

With the increasing construction of large-scale and supertall buildings, the adoption of structural health monitoring (SHM) systems to assess and monitor the safety of various structural components is rapidly increasing [1–3]. In SHM systems, building safety can be evaluated by installing advanced sensors on major structural components to observe changes in responses. The structural response data obtained through advanced sensors in SHM systems contains information that can be extracted and used to evaluate building safety [4–8]. Although various techniques have been developed to extract safety information from structural responses [9–11], system identification (SI) technology is generally used as a representative method. The indices identified by SI technology typically include modal parameters, including natural frequency, mode shape, and modal damping ratio, with these parameters used as indicators of building safety [12–16]. Changes in natural frequency can be used as an indicator to determine whether building safety is deteriorating [17, 18], while changes in mode shape can be used as an indicator to identify locations at which building safety is deteriorating [19, 20]. Furthermore, the modal damping ratio serves as an indicator for determining the dynamic response of a structure during the initial design stage, predicting the system's response to external loads such as earthquakes and wind, and allowing for preassessing the usability of the building to be constructed and the safety of the structure under load. SI technology, which provides important safety evaluation indicators, has been actively used in various industrial fields where safety issues are important due to vibrations, such as civil, mechanical, aviation, and shipbuilding industries [21–23].

SI research for identifying modal parameters has mainly evolved based on frequency domain decomposition (FDD) methods that analyze the structural responses in the

frequency domain [24] and stochastic subspace identification (SSI) methods that analyze them in the time domain [25–28]. The FDD method identifies the natural frequency and mode shape based on the power spectral density (PSD) function of the obtained raw data and identifies the modal damping ratio by performing an inverse Fourier transform on the identified mode frequency components. The SSI method analyzes the raw data to obtain the covariance, constructs a Toeplitz matrix, acquires system matrices A and C through this process, and performs decomposition to identify modal parameters. Both methods represent the frequency and time domains, and SI techniques based on these methods have been developed recently [13, 14, 29, 30]. Kim et al. [31] developed an SI method with computational time advantages using filtered response orthogonality, in which the complex decomposition procedures associated with the FDD method were not required. Park and Oh [32] proposed an SI method that can identify modal parameters in real-time for tall buildings using a filtered response as a target. Yun et al. [33] proposed a minimum condition-based SI method, considering that identification accuracy can be reduced due to the initial setting parameters of FDD. In addition, Xu et al. [34] suggested an SI method that removes harmonic components to use the data, considering that the identification of natural frequencies can be limited due to harmonic components in raw data.

Meanwhile, with the recent developments in system identification (SI) technology, an increasing number of studies have applied deep learning (DL) models [35–37]. DL models use learning-based estimation algorithms between input and output, demonstrating excellent applicability, versatility, and high accuracy performance in various fields, such as image recognition, natural language processing (NLP), speech recognition, and time series prediction [38–40]. Furthermore, DL models acquire information of input data features and discern intricate patterns and relationships, enabling them to make predictions, thus facilitating the modeling of complex nonlinear relationships that are challenging to approach mathematically. As learning occurs in an end-to-end manner, models can be simpler and more efficient; thus, high performance can be expected. Recent efforts have focused on addressing computational time and complexity issues in the SI field using DL models. Kim and Sim [41] developed a DL algorithm that can solve computational time problems by searching for modal frequency peaks in frequency graphs with noise using a region-based convolutional neural network (CNN). Yang et al. [42] proposed a vision-based modal frequency identification technique using CNN and long short-term memory (LSTM). They developed an efficient method for modal parameter identification using the cantilever beam's frame image as input and the natural frequency as output. Mugnaini et al. [43] proposed an SI method that eliminates various spurious modes that occur in the SSI method using statistical principles and machine learning (ML), providing an approach that is objective and completely independent from user experience. Liu et al. [44] proposed a DNN-based modal parameter estimation method, which structured the acceleration response, modal response, and mode shape as input/output relationships. Subsequently, Liu et al. [29] suggested an effective method to address the computational complexity issue by training the future/past output matrix of the SSI method as input and system parameters and a matrix as output using a DNN. In summary, a wide range of DL models, such as ML, DNN, CNN, and LSTM, have been applied in SI technology, leading to ongoing research on identifying modal parameters.

Despite the various SI studies conducted, the problem of identifying modal parameters lies in the instability of identifying the modal damping ratio [45]. Magalhães et al. [45] showed that in the identification of modal damping ratio, FDD-based modal parameter identification becomes less stable than that of natural frequency results. There can be various reasons why the identification stability of the modal damping ratio is not as good as that of the natural frequency, but generally, there are two main causes. First, the use of insufficient measurement data may lead to poor damping ratio results [33, 45]. Yun et al. [33] revealed that because the FDD method assumes ambient vibration responses as white noise input, as the measurement time decreases, modes are not sufficiently excited, the amplitude of the natural frequency decreases, and the identification accuracy of the modal damping ratio reduces. Second, the influence of aerodynamic damping may lead to poor modal damping ratio results. Vortex-induced vibration in the direction perpendicular to the wind direction due to vortex shedding can cause resonance in the structure through lock-in phenomena, leading to aerodynamic damping exhibiting a negative damping ratio [46]. Consequently, the identification of the structure's modal damping ratio may become more unstable [45, 47]. Other factors that may reduce the identification accuracy of the modal damping ratio include nonstationary vibration present in the measurement data and sensor measurement conditions such as sampling frequency. Various hyperparameters used in the FDD method (such as frequency resolution, number of fast Fourier transform (NFFT), window function, and overlap) may also affect the results [48]. Thus, the identification of the modal damping ratio can become more unstable than that of the natural frequency and mode shape due to various reasons [33, 45].

Considering the aforementioned issues in identifying the modal damping ratio, the LSTM algorithm can be a good alternative to address these problems. The LSTM algorithm is a recurrent neural network (RNN)-based model developed for learning time series data [49–52]. It features memory cells and gates to address the long-term dependency problem that arises as the length of the data increases. Therefore, the LSTM model is useful for performing generalized predictions, even for data with significant deviations, by capturing the long-term temporal correlations in the data, suggesting that stable estimation performance can be expected even when the training data contain noise, outliers, or abnormal responses [42]. In fact, various studies have shown that the LSTM model provides stable estimation results even in the presence of noise or outlier data [52, 53]. Thus, the stability properties of LSTM imply that it can solve the instability problem while identifying the modal damping ratio that occurs in the FDD method. In addition,

considering the ability of the LSTM model to handle long-term dependencies, such as in time series data and time-history data, it is considered a reasonable approach for SI techniques that require large amounts of time-history data. Moreover, when considering the complex calculation process of the FDD method, which uses transform functions and decomposition methods and incurs increased computational costs [31, 33], the development of a simplified and efficient LSTM model-based SI technique that directly learns the relationship between acceleration responses acquired from structures and modal parameters is necessary.

This study aims to resolve the instability issue when identifying the modal damping ratio that may arise in the FDD method by proposing an LSTM-based frequency domain decomposition (FDD-LSTM) method that combines FDD with the LSTM model. The FDD-LSTM method uses the acceleration response, which can be acquired from the global behavior of a building, as input data for the LSTM model and outputs the modal parameters. The relationship between input and output is configured as a sequence-to-one LSTM model that receives time series data as input and returns a single output result. This paper is structured as follows. Section 2 provides a brief theoretical introduction to the FDD method and describes the LSTM model. Section 3 analyzes the standard deviation of the proposed FDD-LSTM method and the FDD method using a 3-degrees-of-freedom (3-DOF) numerical analysis model to compare their identification stability. Furthermore, the identification results of modal damping ratio and natural frequency according to the signal-to-noise ratio (SNR) are analyzed to verify whether the proposed FDD-LSTM method exhibits stable identification results even in the presence of noise. Finally, Section 4 validates the identification stability of the proposed FDD-LSTM method using responses acquired from a three-story steel test structure and a supertall building with a height equivalent to 117 stories.

2. Methodology

2.1. Frequency Domain Decomposition. The FDD method acquires modal parameters using ambient vibration responses obtained during building operation because the FDD method assumes ambient vibration responses used for analysis as white noise inputs. Acceleration responses, acquiring which is an easy task, are primarily used as ambient vibration responses, and acceleration responses can be represented by the correlation function according to the following equation:

$$R_{xx}(\tau) = \int_{-\infty}^{\infty} x(t+\tau)x(t)dt. \tag{1}$$

$x(t)$ is the real part signal of the acceleration response, $x(t+\tau)$ is the time lag signal, and τ represents the time lag. The autocorrelation function obtained through equation (1) can be used to construct the PSD function via Fourier transform.

$$S_{xx}(f) = \int_{-\infty}^{\infty} R_{xx}(\tau)e^{-i2\pi f\tau}d\tau. \tag{2}$$

Equation (2) allows the construction of the PSD, which is then used as the element values of the PSD matrix in the FDD. A PSD function is calculated for each esponse acquired at different degrees of freedom. The autospectral density function calculation for the same degree of freedom is real-valued, whereas the cross-spectral density function for different degrees of freedom is calculated as complex-valued. For example, when there is a system with five degrees of freedom, a 5×5 PSD matrix can be created. The length of the PSD function is determined by half the NFFT used. The constructed PSD matrix contains the periodic components of the raw data signal, and by decomposing the complex number-structured PSD matrix using singular value decomposition, the singular values and vectors can be acquired to obtain the natural frequency and mode shape of the structure. The following represents the result of singular value decomposition of the PSD matrix.

$$\mathbf{S}_{xx}(f) = \mathbf{U} \cdot \mathbf{\Sigma} \cdot \mathbf{V}^H. \tag{3}$$

$\mathbf{U}$ and $\mathbf{V}$ are also a unitary matrix and a singular vector matrix, respectively. Generally, the first column of $\mathbf{U}$ represents the mode shape at the frequency resolution Δf. $\mathbf{\Sigma}$ denotes a diagonal matrix with singular values as its elements, and H stands for the Hermitian transpose. The modal assurance criterion (MAC) is calculated using the acquired natural frequency and mode shape. MAC is a measure of the correlation between mode shapes and can be determined through the following equation:

$$\mathrm{MAC} = \frac{\left|\boldsymbol{\varphi}_k^T \boldsymbol{\varphi}_i\right|^2}{\left|\boldsymbol{\varphi}_k^T \boldsymbol{\varphi}_i\right|\left|\boldsymbol{\varphi}_k^T \boldsymbol{\varphi}_i\right|}. \tag{4}$$

When calculating the mode shape vector corresponding to the structure's mode frequency using equation (4), the correlation approaches 1 as the similarity increases. Furthermore, the MAC value decreases as it moves away from the mode frequency. Thus, the sinusoidal wave for identifying the modal damping ratio can be acquired by inverse Fourier transforming (IFT) complex values corresponding to the MAC value standard of 0.7 to 0.9 or higher, and the logarithmic decrement curve can be obtained through equation (1) of the autocorrelation function. More specific methods can be found in the following studies [24, 33, 45, 54].

2.2. Frequency Domain Decomposition Based on LSTM. The LSTM algorithm, proposed by Hochreiter and Schmidhuber [50, 55], was developed for learning time series data. LSTM is an extension of RNN with an added cell state, which solves the gradient vanishing problem that occurs as the length of time series data increases, causing long-term dependencies. Figure 1 illustrates the LSTM unit.

The LSTM unit includes a forget gate, input gate, candidate value, and output gate. Each gate outputs values between 0 and 1 or between −1 and 1 using the sigmoid and hyperbolic tangent functions. These values represent the proportions and degrees of information reflection controlled by each gate. Thus, the LSTM model can selectively maintain

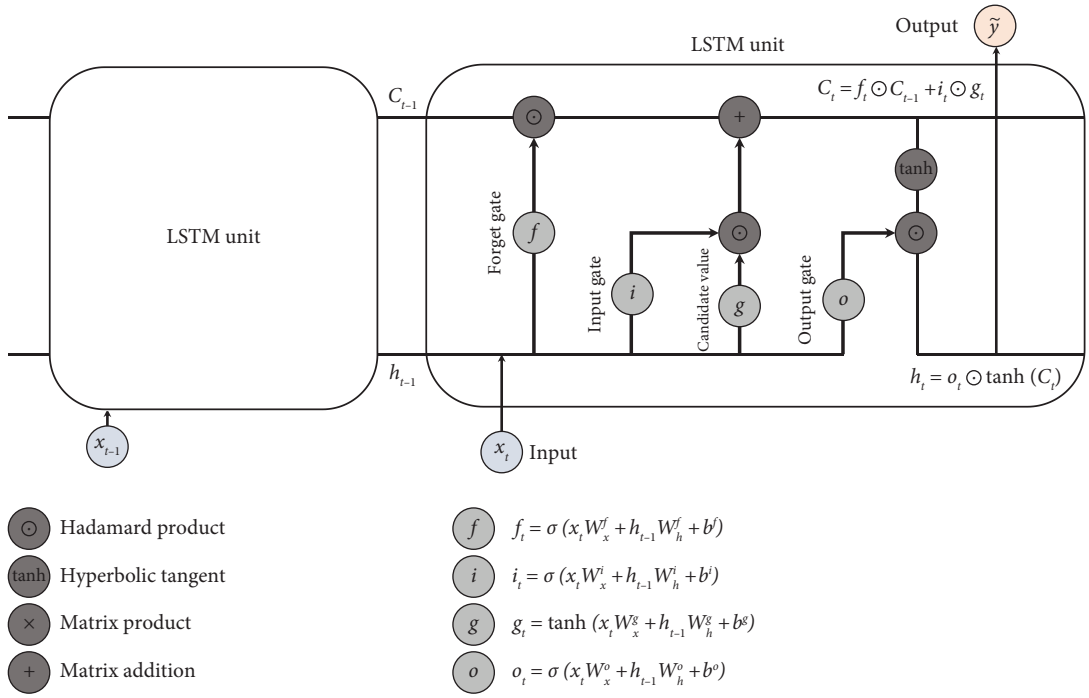

Figure 1: LSTM unit.

or delete important information in long-term sequence data. After passing through the LSTM layer, the calculated predicted output is used to compute the loss function with the target output (output data) as part of weight optimization. The loss function employed in the study is mean square error (MSE), which is calculated in the following equation:

$$\frac{1}{2}\sum_{j=1}^{R}\left(y_j - \tilde{y}_j\right)^2. \tag{5}$$

In equation (5), y represents the target output and $\tilde{y}$ represents the LSTM network's predictions. The target output y corresponds to the modal parameter results identified using the FDD method. R represents the dimensionality of the output. The adaptive moment estimation (Adam) optimizer, introduced by Kingma and Ba [56], was utilized for weight optimization. The updates to the trained network are determined by the following equation:

$$\theta_{t+1} = \theta_t - \frac{\eta}{\sqrt{\widehat{v}_t} + \epsilon}\widehat{m}_t. \tag{6}$$

The parameter θ correspond to the weight and bias, while η represents the learning rate. The variable $\widehat{m}$ denotes the estimates of the first moment (the mean) of the gradients and $\widehat{v}$ represents the second moment (the uncentered variance) of the gradients. The parameter ϵ is proposed with a default value of 10^{-8}. For more detailed information about the Adam optimizer, refer to the following references [56, 57]. The proposed FDD-LSTM method in this study uses acceleration response as input data and modal parameters obtained from the FDD method as output data. Figure 2 shows the configuration of the LSTM structure in the proposed FDD-LSTM method. The input dimension is determined by the system's degrees of freedom, and the time-history structural response is input into the sequence input layer, which is input into the LSTM unit at each time interval Δt. The weight size of the LSTM unit is determined by the number of hidden units, considering the complexity of the model and the amount of information remembered. The loss function is calculated based on the determined modal parameters as the target output, and the LSTM weights are updated by the Adam optimizer.

3. Numerical Verification

3.1. Stability Analysis of the Modal Damping Ratio Obtained from the FDD Method. This section analyzes the identification stability of the natural frequency and modal damping ratios identified by the FDD method. It has been verified whether the identification results follow a normal distribution through probability density functions, and if they do, the standard deviation was used as a stability index [58]. For this process, acceleration responses were obtained from a 3-DOF numerical analysis model. The mass per floor of the 3-DOF model is 5 kg, the floor stiffness is 1000 N/m, and the modal damping ratio is set to 1% for all modes. When the 3-DOF model undergoes eigenvalue decomposition, the natural frequencies appear as 1.0017 Hz, 2.8067 Hz, and 4.0558 Hz. A white noise input load was applied for 2000 s as the excitation load, and the sampling frequency was set to 100 Hz. To identify modal parameters using the FDD method, we used a Hanning window and 50% overlap, with the NFFT set to 200,000. The MAC value criterion was set to 0.8 or higher. Furthermore, under these excitation conditions, a total of 360 sets of acceleration responses and FDD-identified modal parameters were obtained. These datasets

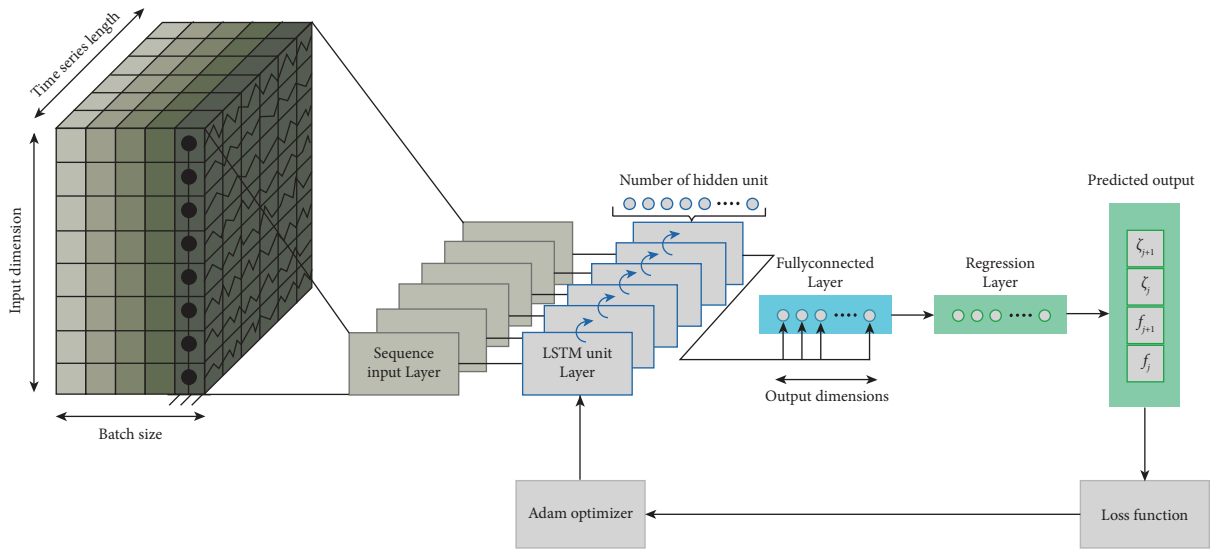

Figure 2: FDD-LSTM structure for the identification of modal parameters.

were used as a training dataset for the subsequent LSTM training. Validation datasets and test datasets were divided into 30 each for verification. The entire dataset comprised 300 training datasets, 30 test datasets, and 30 validation datasets. Figure 3 shows the natural frequency and modal damping ratio results of the first mode of the 300 training datasets identified by the FDD method. As shown in Figure 3, the accurate value of the modal damping ratio is 1%, and the standard deviation for the 300 training datasets is 0.1829. In addition, the accurate natural frequency value is 1.0017 Hz, and the standard deviation for the 300 training datasets is 0.0073. Comparing the magnitudes of the standard deviations and ignoring units, the modal damping ratio's standard deviation appears to be larger than that of the natural frequency, implying that the identification stability of the modal damping ratio is poor. Excluding the influence of aerodynamics, the result is attributed to the use of data with a measurement time of 2000 s, as mentioned in the introduction regarding the instability of the modal damping ratio. Moreover, the initial setting parameters for FDD analysis, such as the window function, overlap ratio, and NFFT, are believed to have caused instability in the identification of the modal damping ratio, indicating that the instability in the identification of the modal damping ratio is indeed higher than that in natural frequency identification. It is unknown whether using measurement data of more than 2000 s would result in better identification stability than the natural frequency because it is well-known that the identification of the modal damping ratio is generally difficult and unstable [33, 45, 47].

Figure 4 shows the probability density function results of the modal damping ratios for each mode. Because all modes from 1 to 3 satisfy a normal distribution, stability evaluation through standard deviation is possible.

Next, LSTM training was conducted with the previously obtained 300 training datasets to examine the stability of the proposed FDD-LSTM method in this study. The hyperparameter settings for training were determined to be

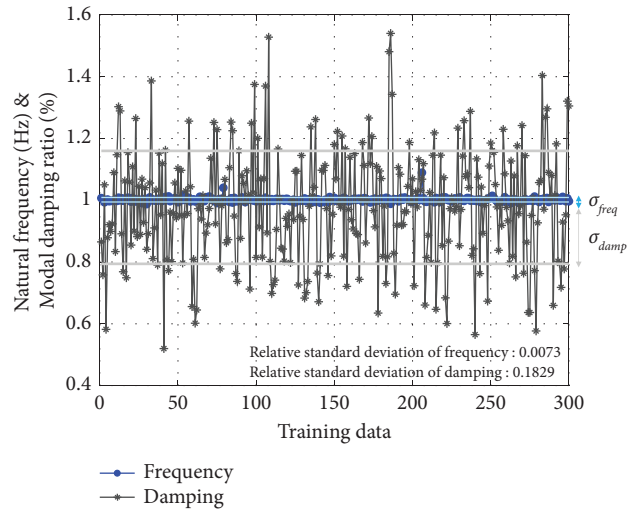

Figure 3: Natural frequency and damping ratio result with respect to 300 training datasets.

a learning rate of 0.0001 and a minibatch size of 100. The maximum number of epochs was set to 1000, and the sequence length was set to 1000. Figure 5 shows the loss function of the training data learned with LSTM. Because the maximum number of epochs is 1000, a total of 600,000 iterations were performed, considering the sequence length, minibatch size, and training dataset. The training loss and validation loss reduce as the training progresses, indicating that LSTM model training was successful.

3.2. Modal Damping Ratio Identified from the FDD-LSTM Method. The test dataset results of the FDD-LSTM method, which was trained with 300 training datasets, are shown in Figure 6. The average modal damping ratio obtained by the FDD-LSTM method was 0.9812%, with a standard deviation of 0.0334%. The average result obtained by the FDD method was 0.9616%, with a standard deviation of 0.2129%. As

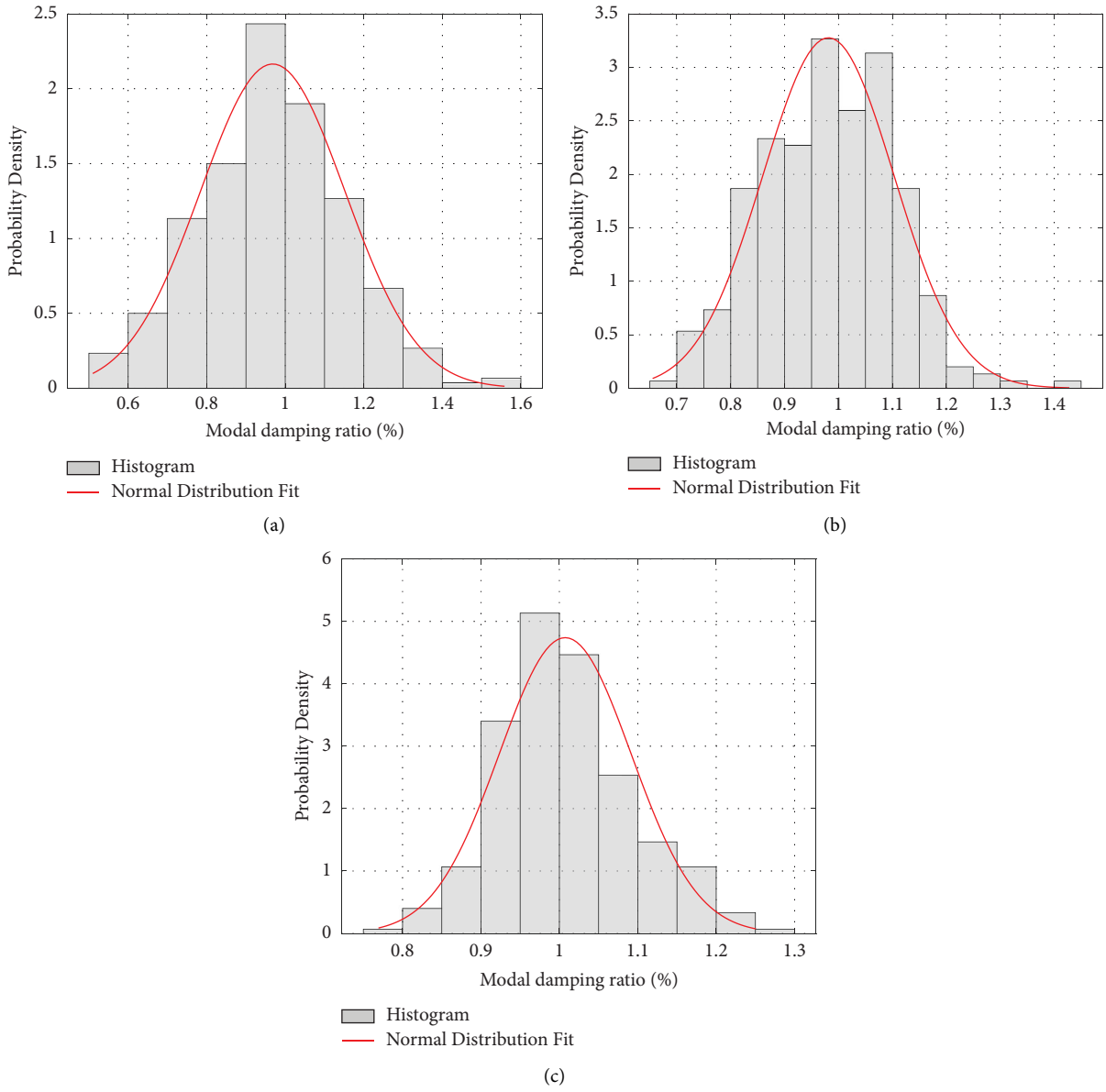

FIGURE 4: Probability density function of the modal damping ratio result with respect to 300 training datasets: (a) 1st mode, (b) 2nd mode, and (c) 3rd mode.

indicated by the identified results, the proposed FDD-LSTM method in this study improved the identification stability compared with the results identified by the FDD method, as it has a smaller standard deviation. In Figure 6(b), the average modal damping ratios of the FDD-LSTM method and the FDD method are 0.9997% and 0.9771%, respectively, with standard deviations of 0.0200% and 0.1295%, respectively. Thus, the standard deviation result of the proposed FDD-LSTM method is lower. Moreover, in Figure 6(c), the averages of the FDD-LSTM method and the FDD method are 1.0246% and 1.0027%, respectively, with standard deviations of 0.0146% and 0.1064%, respectively. The standard deviations are smaller in the 2nd and 3rd modes as well, demonstrating that the FDD-LSTM method exhibits improved identification stability compared to the FDD method. To verify the accuracy of each method, the mean square error (MSE), which is a representative accuracy index, was calculated. The MSEs for the FDD-LSTM and FDD methods were 0.0014% and 0.0453%, respectively. As a smaller MSE indicates better accuracy, this result confirms that the FDD-LSTM method is superior to the FDD method in terms of accuracy. In the 2nd and 3rd modes, the MSEs for each method are 0.00039%, 0.01670%, and 0.00081%, 0.01090%, respectively, showing that the FDD-LSTM method yields better accuracy.

The modal damping ratio results of the test dataset are represented as boxplots. Boxplots are graphs used to evaluate the stability of a model, with the red horizontal line within the box representing the median and the upper and lower horizontal lines of the box representing the 75% and 25% percentiles, respectively. Boxplots can be used to understand

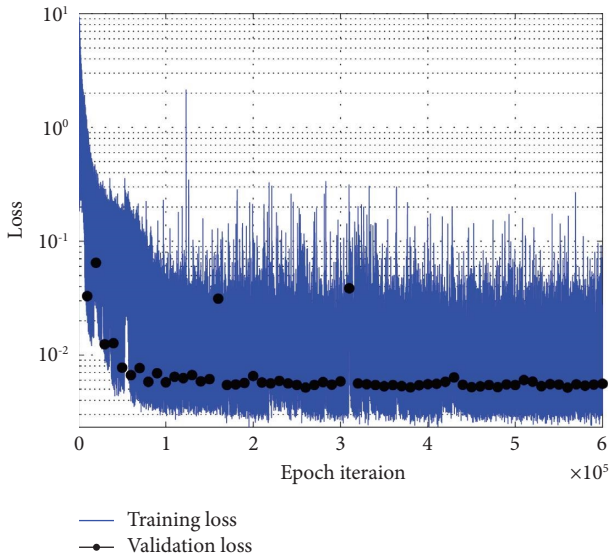

Figure 5: Loss function for training and validation.

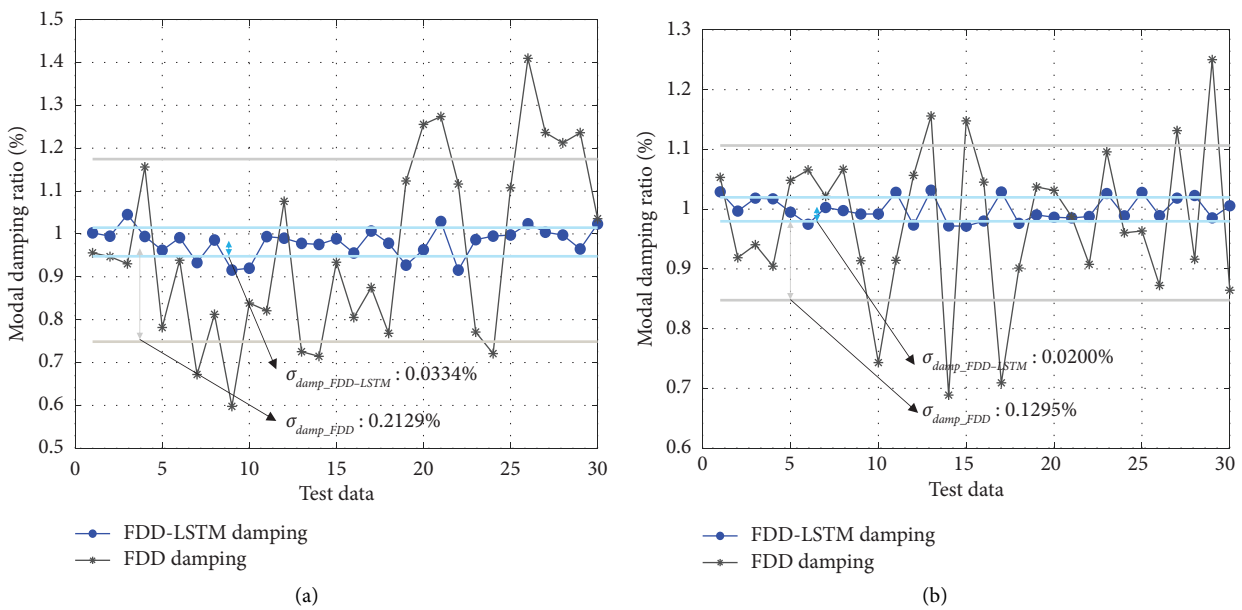

Figure 6: Continued.

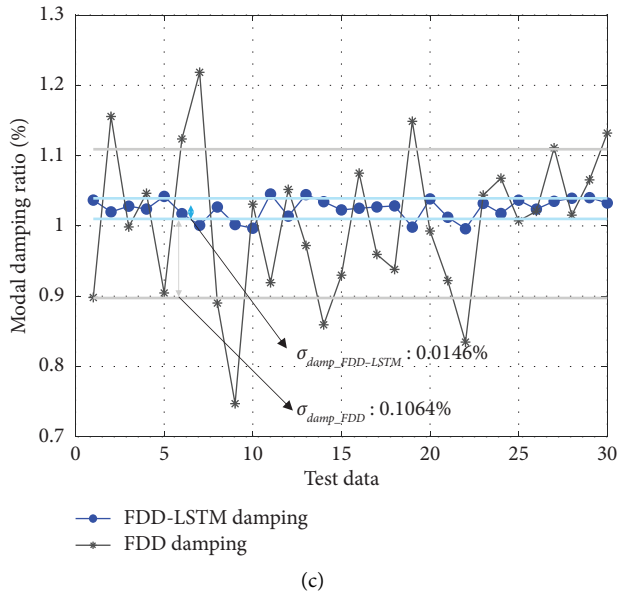

Figure 6: Modal damping ratio prediction of test data using the FDD-LSTM model: (a) 1st mode, (b) 2nd mode, and (c) 3rd mode.

the data distribution and outliers and to compare the stability of different models. The results in Figures 7(a) to 7(c) show that the first quartile ($Q1$) and third quartile ($Q3$) of the FDD-LSTM method, as well as the maximum and minimum values, are located within the interquartile range (IQR) of the FDD method. In the first mode results, the IQR of the FDD-LSTM method is 0.03453%, whereas that of the FDD method is 0.34175%. Moreover, in the second mode, the IQRs are 0.03305% and 0.14891%, respectively, and in the third mode, they are 0.0191% and 0.1455%, respectively. The IQR of the FDD-LSTM method is smaller in all modes, indicating that the stability has been further improved compared to the FDD method.

Figure 8 shows the natural frequency results for the first mode of the test dataset. Unlike the previous modal damping ratio results, no difference in the standard deviation is observed between the FDD method and the FDD-LSTM method, signifying that the results identified by the FDD method in natural frequency identification are consistent and reliable.

3.3. Modal Identification of the FDD-LSTM Method according to Acceleration Data with Noise. This section verifies whether the FDD-LSTM method exhibits satisfactory stability even with noise in the input data. The verification was performed using the 3-DOF model from the previous section, and the stability performance according to the noise was evaluated using the trained FDD-LSTM model without additional training. For this purpose, acceleration responses were obtained from 100 sets with a white noise input load applied to the 3-DOF model, increasing the SNR from 1 to 100 dB. To closely examine the stability at each SNR level, 300 acceleration responses each at the SNR of 80 dB, 60 dB, and 40 dB were obtained. Figure 9 shows the identification results of natural frequency and modal damping ratio as SNR increases. The natural frequency results in Figure 9(a) can be identified as the natural frequency results of the original 3-DOF model at 90 dB and above. At 80 dB and below, the natural frequency identification is relatively widely dispersed compared to that at 90 dB and above, resulting in a large standard deviation and poor stability. Furthermore, the identification results at 80 dB and below show biased estimation and reduced accuracy compared to the results at 90 dB and above. In the modal damping ratio results in Figure 9(b), identification results are generally clustered from 80 dB and above, indicating that stable identification is possible from noise levels of 80 dB and above. Furthermore, there is no biased identification tendency as the SNR decreases, unlike the natural frequency results. In conclusion, as the SNR decreases, the natural frequency shows biased identification results and reduced stability; therefore, the results of the FDD-LSTM method are unreliable below a certain noise level. In contrast, as the SNR decreases, the modal damping ratio increases the standard deviation and reduces the stability but does not show biased identification results, suggesting that the results identified by the FDD-LSTM method can be used below a certain noise level, but the stability needs to be carefully reviewed. A more detailed analysis of the stability performance of the modal damping ratio was conducted using the probability density function at noise levels corresponding to 80 dB, 60 dB, and 40 dB.

Figures 10(a)–10(c) show the probability density function results for the first, second, and third modes at noise levels of 80 dB, 60 dB, and 40 dB, respectively. The stability of the FDD-LSTM method gradually decreases as the noise level increases from 80 dB to 60 dB and 40 dB. The results are consistent with the expectation in Figure 8 that accuracy and stability decrease as the noise level increases. However, even at the largest deviation of the first mode in the FDD-LSTM method, the standard deviation at the 40 dB noise level is

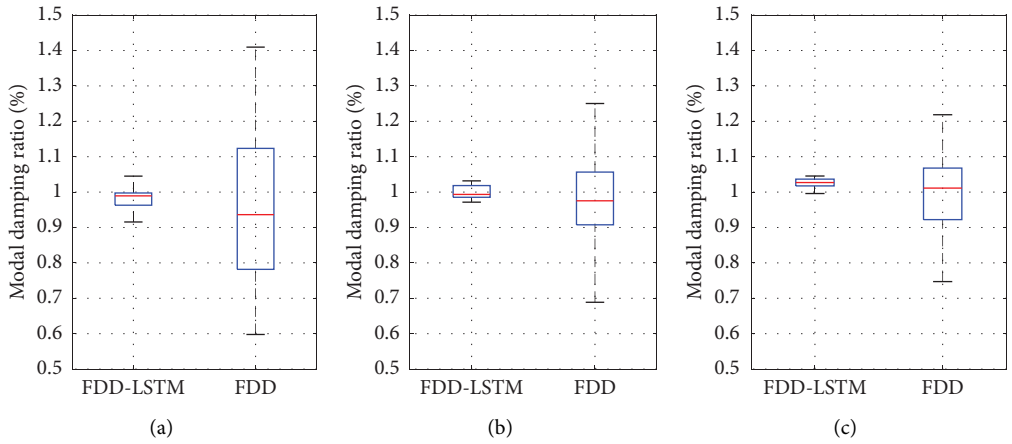

FIGURE 7: Boxplot results of modal damping ratios for each identification method: (a) 1st mode, (b) 2nd mode, and (c) 3rd mode.

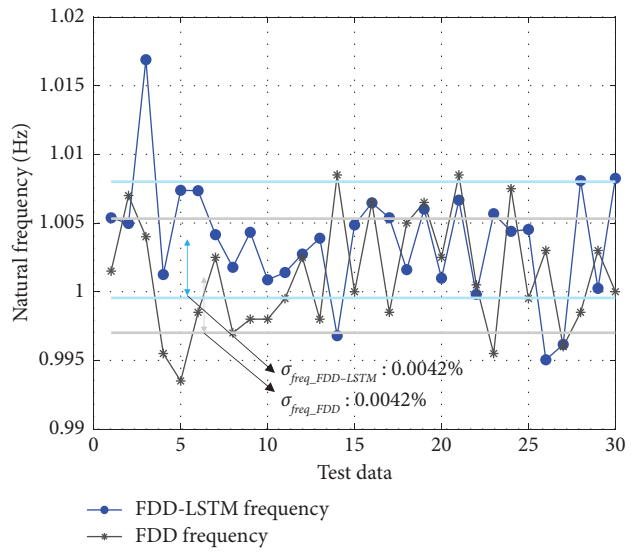

FIGURE 8: Natural frequency prediction results of test data using FDD-LSTM.

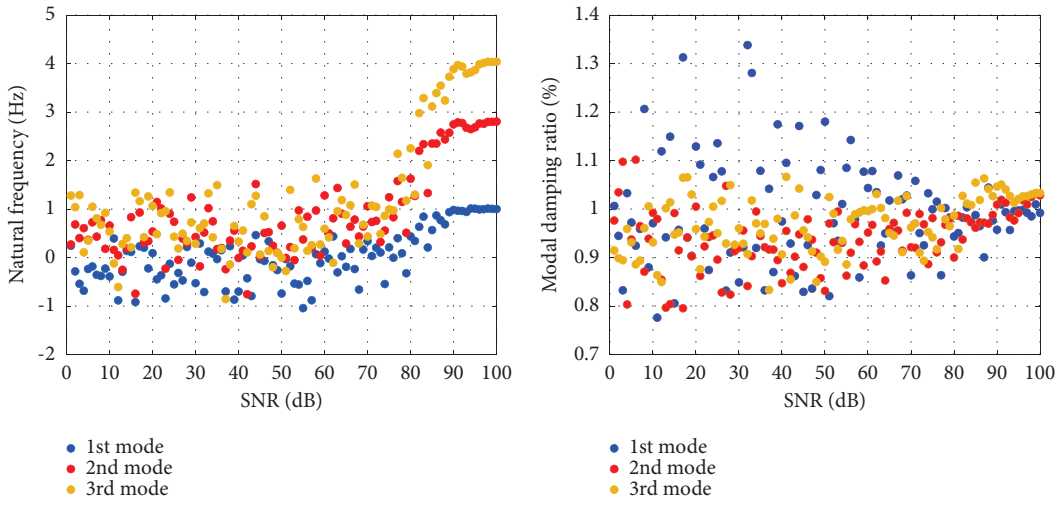

FIGURE 9: Modal parameters of the FDD-LSTM method according to acceleration data with noise: (a) natural frequency and (b) modal damping ratio.

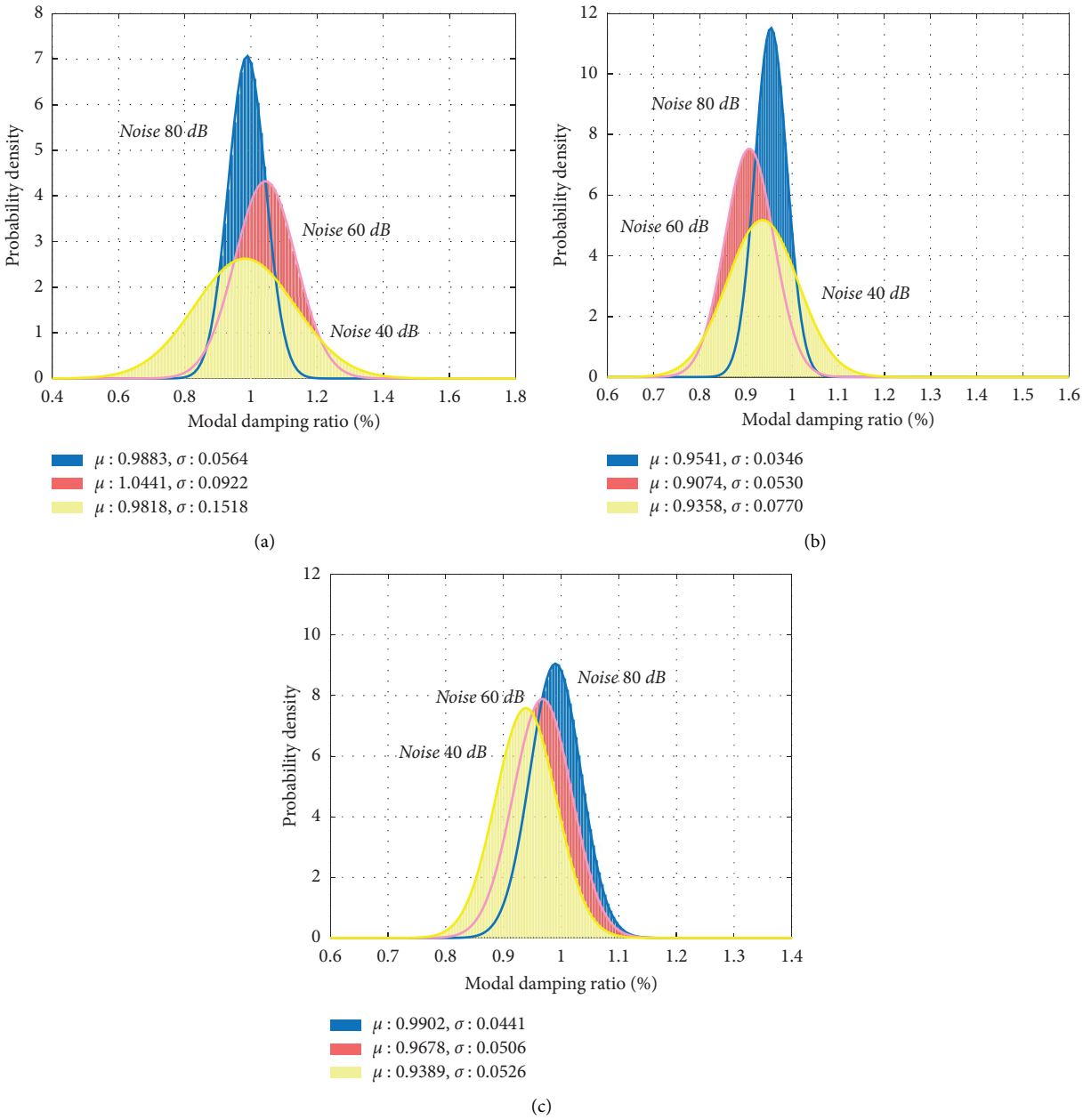

FIGURE 10: Probability density function of FDD-LSTM method according to noise level: (a) 1st mode, (b) 2nd mode, and (c) 3rd mode.

0.1518%, which is lower than the standard deviation of 0.2129% in the FDD method without noise, implying that the FDD-LSTM method can offer better stability performance than the existing FDD method even when noise is present. Furthermore, by examining the identified standard deviation results from the first to the third mode, it is evident that the rate of increase in the standard deviation decreases as the mode increases, indicating that higher-order modes are less affected by noise. In fact, considering the results in Figure 7 of Section 3.2, where the IQR of the third mode was the smallest, it can be inferred that the stability of the third mode was the best and the impact of noise was the smallest. The accuracy indicator, MSE, decreases in the first mode in the order of SNR 80 dB, 60 dB, and 40 dB, with values of 0.0032, 0.0102, and 0.0209, respectively. The MSE results increased because the standard deviation, representing stability, increased with the noise level. In the stability evaluation according to the noise level, the proposed FDD-LSTM method yielded lower standard deviation results than the FDD method. Thus, by utilizing the LSTM model, the proposed method effectively solves the instability problem in the modal damping ratio even when noise is present.

4. Experimental Study

4.1. Verification of the FDD-LSTM Method through the Three-Steel Frame Model. The identification stability of the FDD-LSTM method was verified using a three-story steel frame model. Figure 11 shows the plan view, elevation view, and actual photo of the three-story steel frame model. To measure the dynamic response of the three-story steel frame specimen, measurements were taken in the long side direction, which is the X-direction without braces attached, and the vibration in the Y-direction was minimized by attaching braces. A PCB 333B30 model accelerometer with a sensitivity of 100 mV/g was used as the measurement acceleration sensor, and an IOTECH 4-channel logger was used as the data acquisition device. The sampling frequency for measurement was set to 256 Hz, and the ambient vibration response was measured for approximately 60 h to construct training data. The free vibration response was also acquired, and the modal damping ratios corresponding to the first to third modes were identified. The free vibration response was measured by artificially displacing the top of the three-story steel frame with a thread and then cutting the thread.

Figure 12 shows the mode shapes of the three-story steel frame specimen. The mode shapes were obtained using the FDD method, with the first mode identified at approximately 4.00 Hz, the second at 11.68 Hz, and the third at 17.51 Hz. Because the mode shape results at the identified natural frequencies represent the unique deformation shapes of the first to third modes, it can be judged that the specimen's modes up to the third mode were appropriately identified.

Magalhães et al. [45] recommend the use of free vibration responses to accurately identify the modal damping ratios, stating that the FDD method's modal damping ratio results using free vibration responses provide reliable identification results. Figure 13 shows the modal damping ratio results obtained using the FDD method with the free vibration response. The modal damping ratios at each mode were obtained through exponential function fitting, and the first to third modes were identified as 0.14%, 0.09%, and 0.09%, respectively. These results are used as reference results for the three-story steel frame specimen in the subsequent accuracy comparison of the FDD-LSTM method.

Next, to construct the LSTM model for the FDD-LSTM method, data measured for 60 h were divided into 30 min datasets to create the X and Y training datasets. A total of 120 datasets were constructed, of which 100 were used for training and 20 for testing. The hyperparameters used for training were determined to be a minibatch size of 20, a maximum number of epochs of 2000, a sequence length of 2000, and a learning rate of 0.0001. Figure 14 shows the identification results of the modal damping ratio for the 20 test datasets of the FDD-LSTM method. The identified standard deviation results for the FDD-LSTM method were identified in the order from the first to third modes as 6.7606×10^{-6}%, 1.4398×10^{-4}%, and 6.8690×10^{-5}%, and for the FDD method as 6.0604×10^{-4}%, 3.2848×10^{-4}%, and 2.4686×10^{-4}%, respectively. The FDD-LSTM method identifies the modal damping ratio with relatively consistent results compared to the FDD method, and the standard deviation results show smaller values than the FDD method, indicating improved identification stability. Because there are no outliers, anomalies, or abnormal results in the identified results using the FDD-LSTM method, the mean results can be used as an accuracy indicator, and the average results of the modal damping ratios from the first to third modes are identified as 0.1422%, 0.1037%, and 0.0966%, respectively. The results using the free vibration response in Figure 13 show a difference of less than approximately 0.02% in the second mode. The proposed FDD-LSTM method demonstrates satisfactory performance for both stability and accuracy in the verification using the three-story steel frame specimen.

4.2. Verification of FDD-LSTM Method through Supertall Building with 117 Floors. The identification stability of the FDD-LSTM method was verified using the acceleration response of a supertall building with 117 stories. For this purpose, acceleration response measurements were taken at the top floor for approximately 84 h. The accelerometer used was GioSIG's AC-73, with a full-scale range of 0.5 g, sensitivity of 20 V/g, and a sampling frequency of 100 Hz. Figure 15 shows the floor plan of the supertall building and the sensor locations. To measure the X-axis direction mode through ch1 and the torsional mode through ch2, the sensors were installed as shown in Figure 15(b).

Figure 16(a) shows the natural frequencies of the first to third modes identified through the acquired structural response. The PSD results of the data measured at the top floor are presented; because measurements were only performed in the X-axis direction, it is not possible to know if the first to third frequency peaks include torsional modes. However, as shown in Figure 16(b), torsion is observed in the mode shape phase on the same plane, suggesting that the second mode is a torsional mode. Furthermore, since the third mode shows the same mode shape phase in the same plane, it can be assumed to be the second mode along the X-axis. In real buildings, it is impossible to obtain free vibration responses, so modal damping ratios must be identified using as much measured data as possible, and these results should be used as reference values. When identifying the modal damping ratios using all the data measured for 84 h, the first to third modes are identified as 0.0075, 0.0076, and 0.0075, respectively.

The measurement data corresponding to 84 h, which is approximately 30,000,000 data points, were divided into 300,000 data segments, and the FDD method was employed. A total of 80 training datasets and 20 test datasets were constructed. The hyperparameter setting for LSTM training is the same as the steel frame specimen in Section 4.1. Figure 17 shows the identification results of the modal damping ratio for the 20 test datasets. As shown in the legend of Figure 17, the standard deviation results of the FDD-LSTM method are smaller than those of the FDD method in all modes from the first to third. Indeed, compared with the irregular identification results of the FDD method in Figures 17(a) to 17(c), the FDD-LSTM method

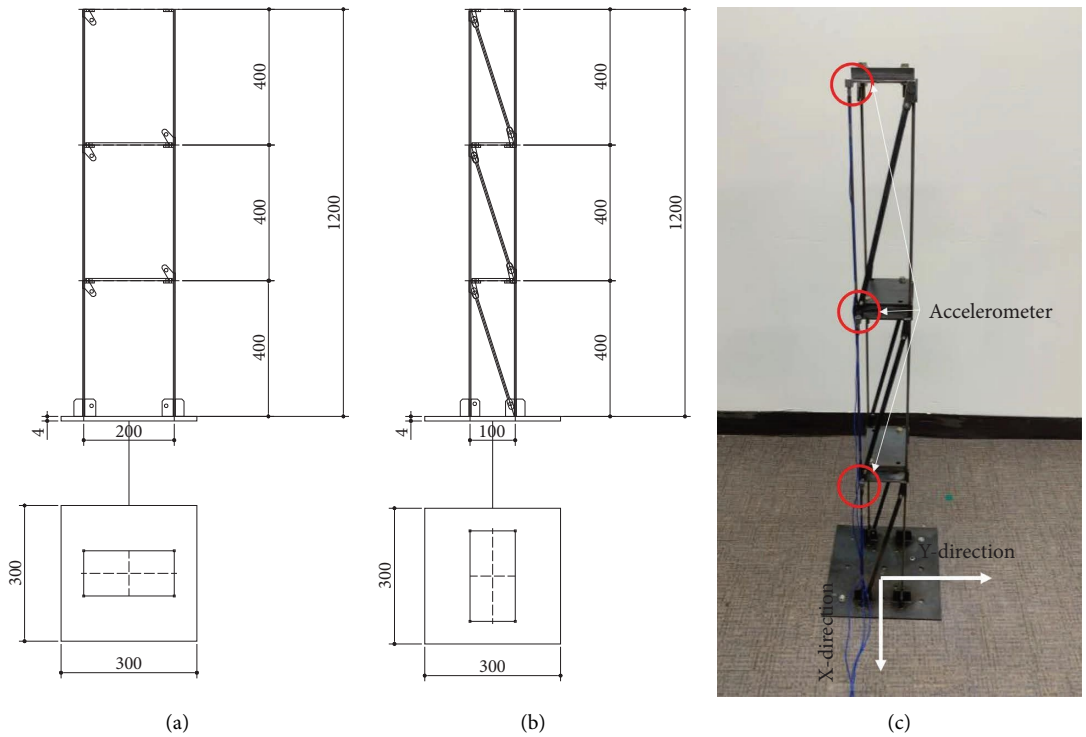

Figure 11: Three-story steel frame model: (a) front view, (b) side view, and (c) aerial view.

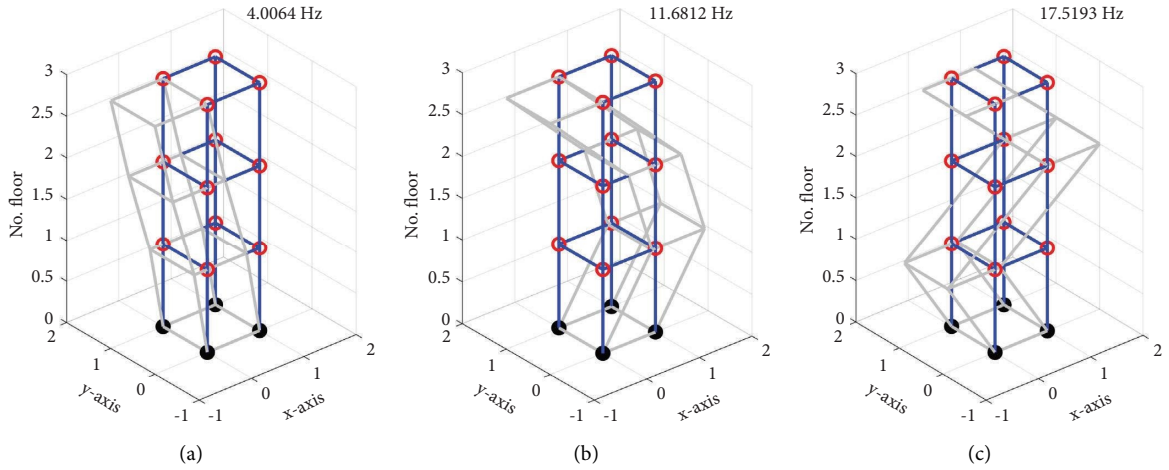

Figure 12: Mode shape: (a) 1st mode, (b) 2nd mode, and (c) 3rd mode.

provides stable identification results. Moreover, the FDD-LSTM method shows average results of 0.0075, 0.0076, and 0.0079 for the first to third modes, with a maximum relative error difference of about 5% compared to the reference result in the third mode. Considering the difference at the fourth decimal place, it is deemed an acceptable relative error result. As such, the FDD-LSTM method enables stable estimation by generalizing the unstable identification results shown by the FDD method based on a large amount of data.

The proposed FDD-LSTM method was compared with the time-domain identification technique of SSI-Covariance (COV). The SSI-COV method constructs the structural response as a block Toeplitz matrix and decomposes it to form a system matrix, thereby identifying the modal parameters. To obtain reliable results for modal parameters, all 84 hours of measured data were utilized. For the initial settings of SSI–COV, the model order was set to 100, the number of block rows was set to 40, and the stabilization criterion was set to $\mathrm{d}f = 0.01$, $\mathrm{d}\zeta = 0.05$, MAC = 0.90. Further details about the SSI-COV method can be found in the papers by Peeters and De Roeck [25, 26]. Figure 18 presents the stabilization diagram and the results for the modal damping ratio. In addition, Table 1 summarizes the results from the previously identified FDD-LSTM, FDD, and SSI-COV methods. In Figure 18(a), stable poles appear at approximately 0.13 Hz, 0.20 Hz, and 0.30 Hz as identified by the FDD method.

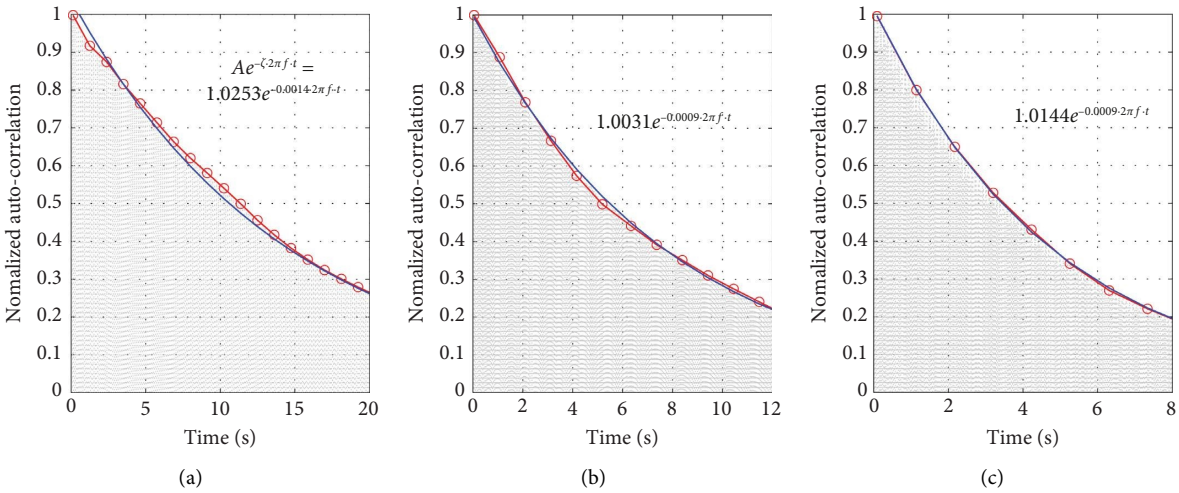

Figure 13: Modal damping ratio: (a) 1st mode, (b) 2nd mode, and (c) 3rd mode.

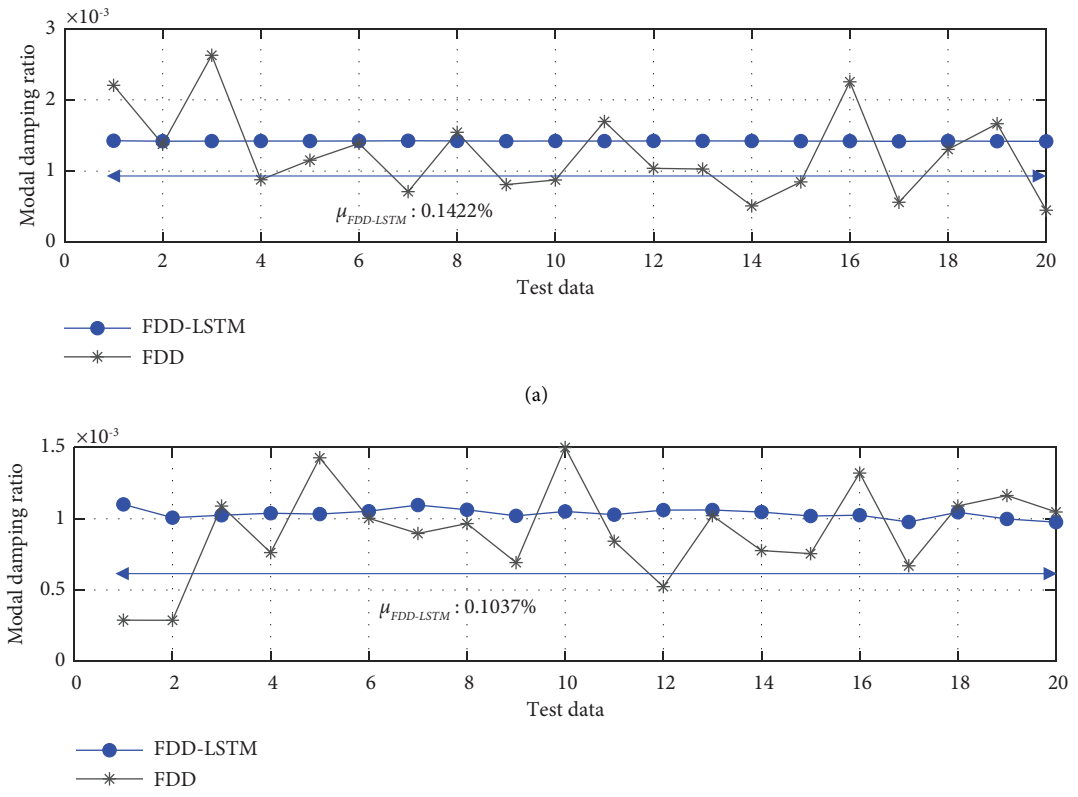

Figure 14: Continued.

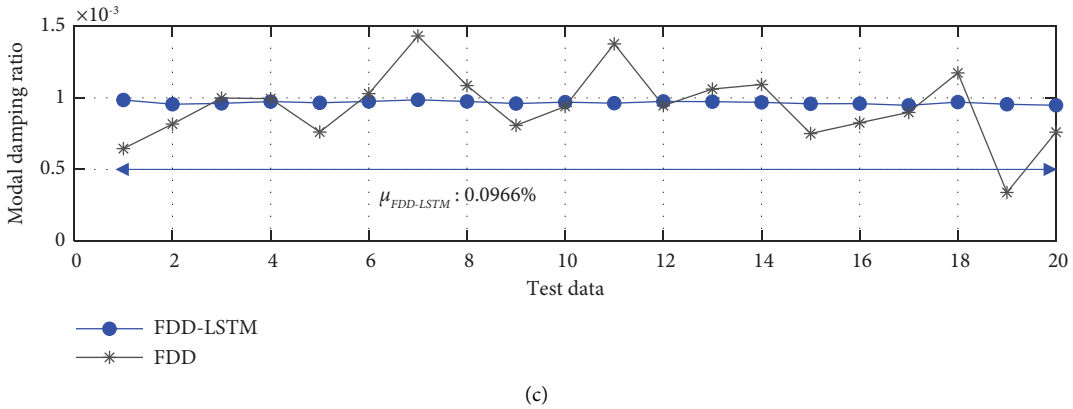

(c)

FIGURE 14: Modal damping ratios for the test data of FDD-LSTM: (a) 1st mode, (b) 2nd mode, and (c) 3rd mode.

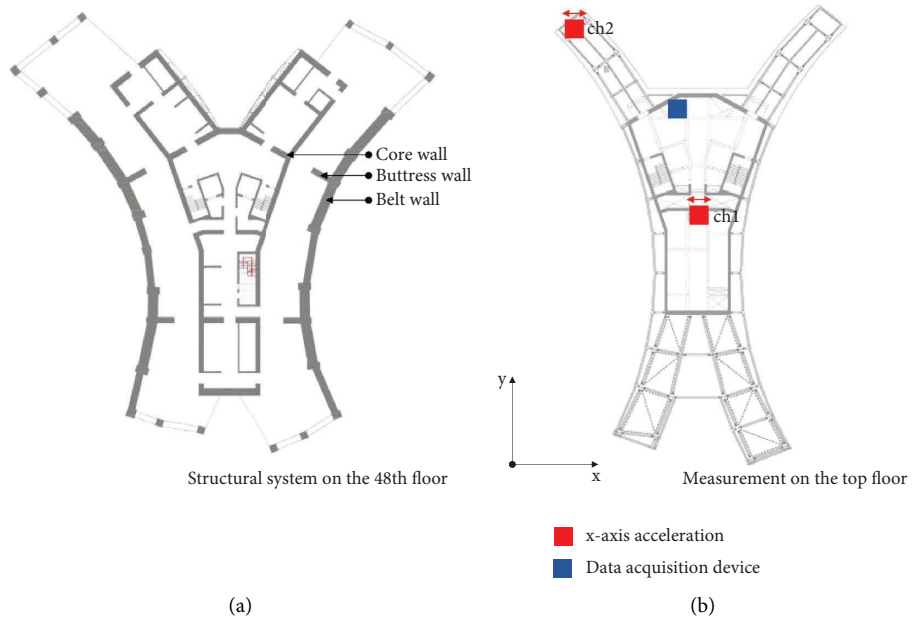

(a) (b)

FIGURE 15: Plan view and measurement location: (a) 48th floor and (b) top floor.

Figure 18(b) displays the modal damping ratio results at each stable pole. The first mode from the FDD-LSTM and FDD methods differs by about 0.002 in the modal damping ratio compared to the average results of the SSI-COV method. This is supposed to be the result of differences in interpretation between the frequency domain and the time domain. Moreover, while the standard deviation for the first mode in the SSI-COV method is lower than that of the FDD-LSTM method, the latter shows higher values for the second and third modes. This implies that the SSI-COV method becomes less stable as it identifies higher modes. In contrast, the FDD-LSTM method demonstrates less variability in the standard deviations for the first to third modes, indicating stability even for higher modes. Therefore, the FDD-LSTM method, trained on a large dataset, can be expected to provide more stable identification than existing SI methods.

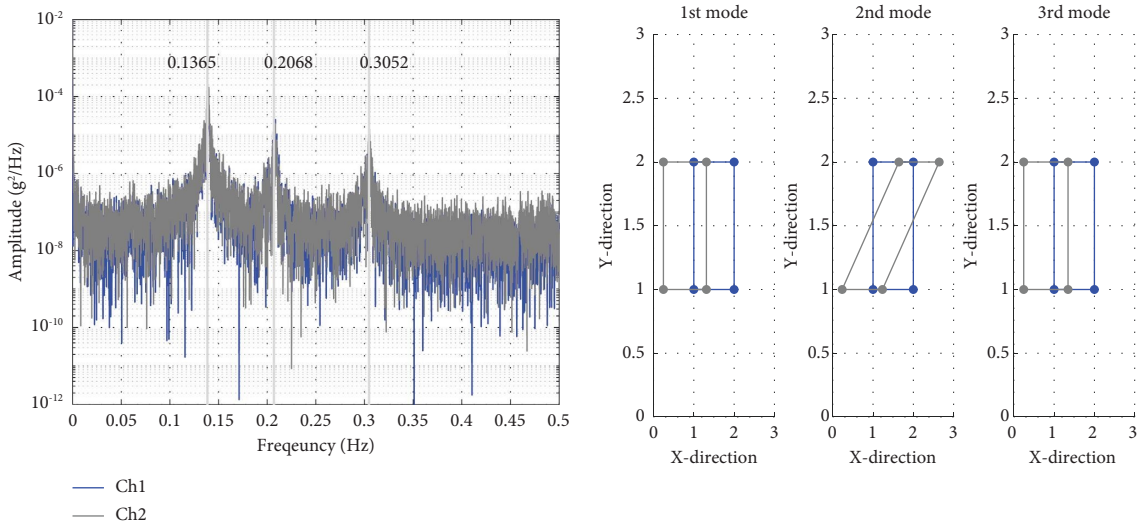

(a) (b)

Figure 16: Modal parameters through FDD: (a) natural frequency and (b) mode shape.

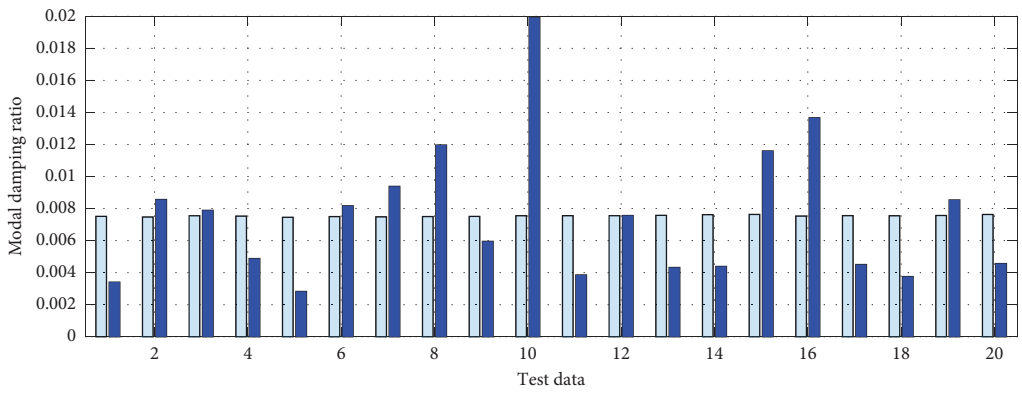

(a)

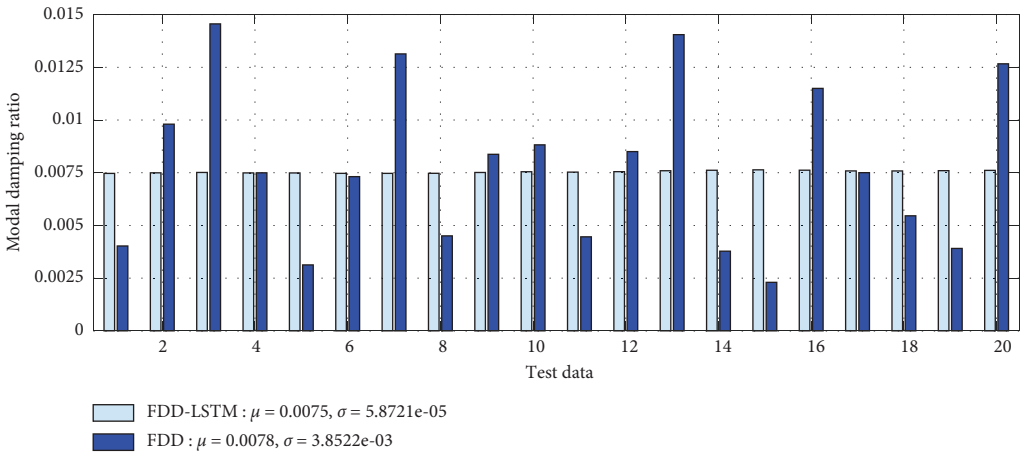

(b)

Figure 17: Continued.

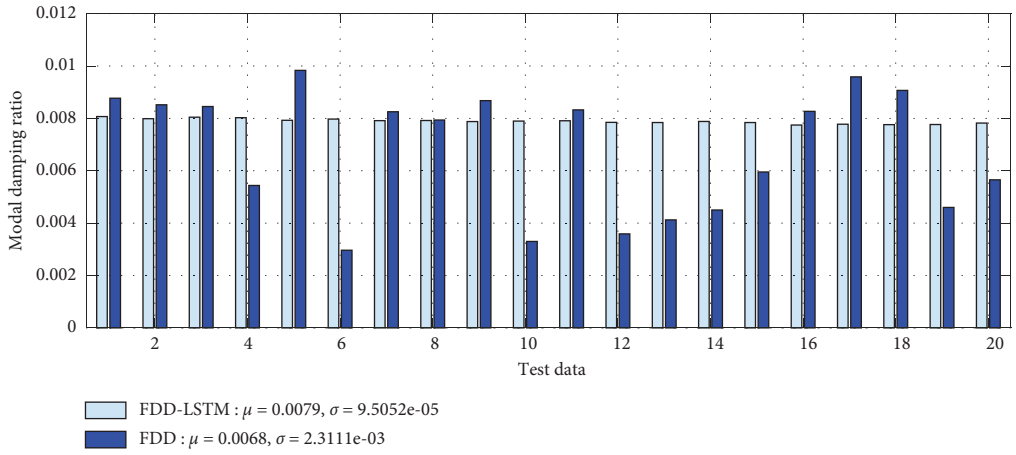

(c)

Figure 17: Modal damping ratios for test data of FDD-LSTM: (a) 1st mode, (b) 2nd mode, and (c) 3rd mode.

Table 1: Comparison of results for each system identification method.

Methods	Mode					
	1st		2nd		3rd	
	μ	σ	μ	σ	μ	σ
FDD-LSTM	0.0075	$9.3983e-05$	0.0075	$5.8721e-05$	0.0079	$9.5052e-05$
FDD	0.0075	$4.2804e-03$	0.0078	$3.8522e-03$	0.0068	$2.3111e-03$
SSI-COV	0.0056	$4.6686e-05$	0.0071	$1.1853e-04$	0.0066	$2.7249e-04$

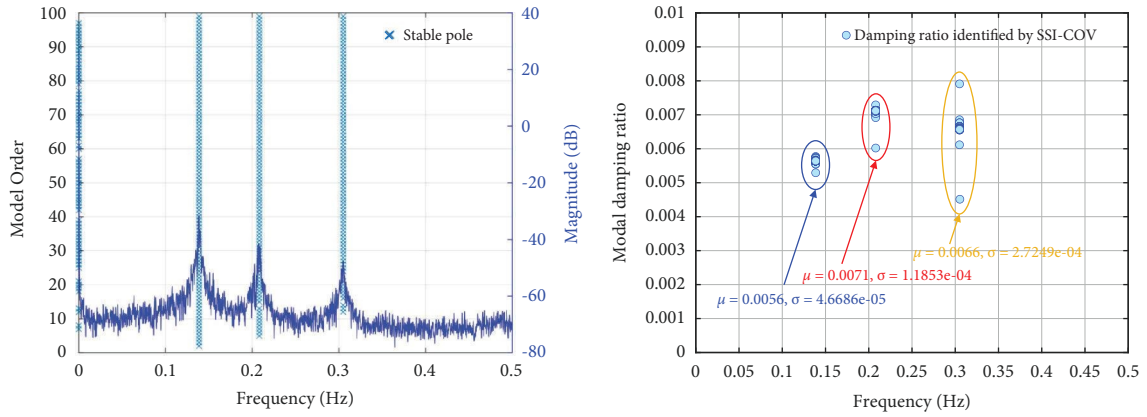

(a) (b)

Figure 18: Modal parameters identified by SSI-COV: (a) stabilization diagram and (b) modal damping ratio.

5. Conclusion

This study proposed the FDD-LSTM method, which applies the LSTM model to the FDD method, to address the instability issue of modal damping ratio identification by the FDD method. The FDD method has the disadvantage of producing unstable identification results due to changes in the modal damping ratio caused by measurement time, initial settings, and abnormal responses in the measured data. To overcome this issue, the LSTM model, which is a type of DL model, was applied to address the instability issue in the FDD method. The FDD-LSTM method enables generalized estimation based on a large amount of data and resolves the instability problem of the FDD method. This improvement can be attributed to the inherent characteristics of LSTM models, which include their ability to handle time dependency, provide temporal smoothing, and learn patterns. All the data used, including the x input data, can be temporally connected using the stateful functionality of LSTM, enabling stable estimation even in cases with

substantial variability. The proposed FDD-LSTM method was validated using a 3-DOF numerical model, a three-story steel frame specimen, and a 117-story supertall building.

In the 3-DOF numerical model, the standard deviation results for the first to third modes were smaller for the FDD-LSTM method than for the FDD method, indicating improved stability. Moreover, in the stability verification based on noise levels, the FDD-LSTM method exhibited a standard deviation of 0.1518% at a noise level of 40 dB, which was lower than the 0.2129% result of the FDD method without noise. Consequently, even with 40 dB of noise in the raw data, the FDD-LSTM method demonstrated better safety performance than the FDD method. However, biased identification results were observed for natural frequency depending on the noise level, necessitating further analysis in future research. In the three-story steel frame specimen, the proposed method yielded lower standard deviation results in all modes from the first to third compared to the FDD method. Furthermore, in the modal damping ratio results obtained through free vibration response, the FDD-LSTM method showed superior accuracy along with stability, displaying a maximum difference of less than 0.02% in the second mode. In the supertall building validation, the FDD-LSTM method also showed improved stability with lower standard deviation results in the identified modes compared to the FDD method and exhibited satisfactory accuracy, exhibiting a maximum relative error difference of ~5%. In comparison with existing SI methods, it was confirmed that the FDD-LSTM method is capable of stable estimation even for higher-order modes.

As the FDD-LSTM method proposed in this study is based on the modal damping ratio results obtained from the FDD method to construct the training dataset, it is considered highly dependent on the identification results of the FDD method. It was confirmed that if the FDD method does not provide biased identification results and stability is degraded, then stability can be improved through the proposed FDD-LSTM method. However, in this study, it is assumed that the modal parameters of the building do not change due to structural damage. Therefore, in the future, it will be necessary to verify whether the proposed method can provide stable estimation results even when structural damage occurs. In addition, it will be necessary to acquire structural responses from various supertall buildings and identify modal damping ratios to provide generalized identification performance for the proposed FDD-LSTM method. Through this process, it is expected to develop an integrated model for the stable identification of modal damping ratios that provides generalized identification results for all supertall structures.

Data Availability

The dataset used in this study is not available for public access due to contractual or agreement restrictions, preventing the disclosure of the data.

Conflicts of Interest

The authors declare that they have no conflicts of interest.

Acknowledgments

This work was supported by a National Research Foundation of Korea (NRF) and Grant was funded by the Korea Government (Ministry of Science, ICT & Future Planning, MSIP) (NRF-2021R1A2C33008989 and No. 2018R1A5A1025137).

References

[1] M. Civera, V. Mugnaini, and L. Zanotti Fragonara, "Machine learning-based automatic operational modal analysis: a structural health monitoring application to masonry arch bridges," *Structural Control and Health Monitoring*, vol. 29, no. 10, 2022.

[2] M. Mousavi, A. H. Gandomi, M. Abdel Wahab, and B. Glisic, "Monitoring onsite-temperature prediction error for condition monitoring of civil infrastructures," *Structural Control and Health Monitoring*, vol. 29, no. 12, 2022.

[3] B. K. Oh, S. H. Lee, and H. S. Park, "Damage localization method for building structures based on the interrelation of dynamic displacement measurements using convolutional neural network," *Structural Control and Health Monitoring*, vol. 27, no. 8, 2020.

[4] W. H. Hu, Z. M. Xu, X. H. Bian et al., "Operational modal analysis and continuous dynamic monitoring of high-rise building based on wireless distributed synchronized data acquisition system," *Structural Control and Health Monitoring*, vol. 29, no. 11, 2022.

[5] M. Impraimakis and A. W. Smyth, "Input–parameter–state estimation of limited information wind-excited systems using a sequential Kalman filter," *Structural Control and Health Monitoring*, vol. 29, no. 4, 2022.

[6] J. Shan, L. Wang, C. N. Loong, and Z. Zhou, "Rapid seismic performance evaluation of existing frame structures using equivalent SDOF modeling and prior dynamic testing," *Journal of Civil Structural Health Monitoring*, vol. 13, no. 2-3, pp. 749–766, 2023a.

[7] J. Shan, C. Zhuang, and C. N. Loong, "Parametric identification of Timoshenko-beam model for shear-wall structures using monitoring data," *Mechanical Systems and Signal Processing*, vol. 189, Article ID 110100, 2023b.

[8] Y. Yang, M. Chadha, Z. Hu, and M. D. Todd, "An optimal sensor placement design framework for structural health monitoring using Bayes risk," *Mechanical Systems and Signal Processing*, vol. 168, Article ID 108618, 2022.

[9] K. Huang, K. V. Yuen, L. Wang, T. Jiang, and L. Dai, "Ensor fault detection, localization, and reconstruction for online structural identification," *Structural Control and Health Monitoring*, vol. 52, pp. 1–22, 2022.

[10] H. S. Park and B. K. Oh, "Damage detection of building structures under ambient excitation through the analysis of the relationship between the modal participation ratio and story stiffness," *Journal of Sound and Vibration*, vol. 418, pp. 122–143, 2018.

[11] Y. Xia, X. Lei, P. Wang, G. Liu, and L. Sun, "Long-term performance monitoring and assessment of concrete beam

bridges using neutral axis indicator," *Structural Control and Health Monitoring*, vol. 27, no. 12, 2020.

[12] M. H. Abdelbarr, M. D. Kohler, and S. F. Masri, "Structural identification of a 52-story high-rise in downtown Los Angeles based on short-term wind vibration measurements," *Journal of Structural Engineering*, vol. 149, no. 1, Article ID 05022002, 2023.

[13] Z. R. Lu, G. Lin, and L. Wang, "Output-only modal parameter identification of structures by vision modal analysis," *Journal of Sound and Vibration*, vol. 497, Article ID 115949, 2021.

[14] D. Y. Yun, H. B. Shim, and H. S. Park, "SSI-LSTM network for adaptive operational modal analysis of building structures," *Mechanical Systems and Signal Processing*, vol. 195, Article ID 110306, 2023.

[15] D. Y. Yun and H. S. Park, "Accuracy and stability evaluation of modal damping ratio identification techniques for high-rise buildings," *Journal of the Architectural Institute of Korea*, vol. 36, no. 8, 2020.

[16] D. Y. Yun and H. S. Park, "Modal identification of building structures under unknown input conditions using extended Kalman filter and long-short term memory," *Integrated Computer-Aided Engineering*, vol. 30, no. 2, pp. 185–201, 2023.

[17] Y. Fang, X. Liu, J. Xing, Z. Li, and Y. Zhang, "Substructure damage identification based on sensitivity of Power Spectral Density," *Journal of Sound and Vibration*, vol. 545, Article ID 117451, 2023.

[18] F. Shadan, F. Khoshnoudian, and A. Esfandiari, "A frequency response-based structural damage identification using model updating method," *Structural Control and Health Monitoring*, vol. 23, no. 2, pp. 286–302, 2016.

[19] L. Ma, C. S. Cai, L. H. Wu, and S. F. Li, "Study on the dynamic characteristics of the suspender with additional dampers and a frequency-based multiple parameter identification method for the system," *Journal of Sound and Vibration*, vol. 553, Article ID 117660, 2023.

[20] K. Roy, "Structural damage identification using mode shape slope and curvature," *Journal of Engineering Mechanics*, vol. 143, no. 9, pp. 1–12, 2017.

[21] Y. Lee, G. Lee, D. S. Moon, and H. Yoon, "Vision-based displacement measurement using a camera mounted on a structure with stationary background targets outside the structure," *Structural Control and Health Monitoring*, vol. 29, no. 11, 2022.

[22] J. X. Mao, H. Wang, Y. G. Fu, and B. F. Spencer, "Automated modal identification using principal component and cluster analysis: application to a long-span cable-stayed bridge," *Structural Control and Health Monitoring*, vol. 26, no. 10, 2019.

[23] J. Yang, R. Zhu, H. P. Lee, M. Li, and X. Yin, "Experimental and numerical dynamic analysis of marine herringbone planetary gearbox supported by journal bearings," *Journal of Sound and Vibration*, vol. 545, Article ID 117426, 2023.

[24] R. Brincker, C. E. Ventura, and P. Andersen, "Damping estimation by frequency domain decomposition," *Proceedings of the International Modal Analysis Conference- IMAC*, vol. 1, pp. 698–703, 2001.

[25] B. Peeters and G. De Roeck, "Reference-based stochastic subspace identification for output-only modal analysis," *Mechanical Systems and Signal Processing*, vol. 13, no. 6, pp. 855–878, 1999.

[26] B. Peeters and G. De Roeck, "Stochastic system identification for operational modal analysis: a review," *Journal of Dynamic Systems, Measurement, and Control*, vol. 123, no. 4, pp. 659–667, 2001.

[27] P. Van Overschee, B. De Moor, P. V. Overschee, and B. D. Moor, "Subspace identification for linear system: theory-implementation- applications," in *Proceedings of the International Conference of IEEE Engineering in Medicine and Biology Society*, Sydney, Australia, June 2008.

[28] P. Van Overschee and B. De Moor, "Subspace algorithms for the stochastic identification problem," *Automatica*, vol. 29, no. 3, pp. 649–660, 1993.

[29] D. Liu, Y. Bao, and H. Li, "Machine learning-based stochastic subspace identification method for structural modal parameters," *Engineering Structures*, vol. 274, Article ID 115178, 2023.

[30] M. Makki Alamdari, A. Anaissi, N. L. D. Khoa, and S. Mustapha, "Frequency domain decomposition-based multisensor data fusion for assessment of progressive damage in structures," *Structural Control and Health Monitoring*, vol. 26, no. 2, p. e2299, 2019.

[31] D. Kim, B. K. Oh, H. S. Park, H. B. Shim, and J. Kim, "Modal identification for high-rise building structures using orthogonality of filtered response vectors," *Computer-Aided Civil and Infrastructure Engineering*, vol. 32, no. 12, pp. 1064–1084, 2017.

[32] H. S. Park and B. K. Oh, "Real-time structural health monitoring of a supertall building under construction based on visual modal identification strategy," *Automation in Construction*, vol. 85, pp. 273–289, 2018b.

[33] D. Y. Yun, D. Kim, M. Kim et al., "Field measurements for identification of modal parameters for high-rise buildings under construction or in use," *Automation in Construction*, vol. 121, Article ID 103446, 2021.

[34] M. Xu, F. T. K. Au, S. Wang, and H. Tian, "Operational modal analysis under harmonic excitation using Ramanujan subspace projection and stochastic subspace identification," *Journal of Sound and Vibration*, vol. 545, Article ID 117436, 2023.

[35] O. Abdeljaber, O. Avci, S. Kiranyaz, M. Gabbouj, and D. J. Inman, "Real-time vibration-based structural damage detection using one-dimensional convolutional neural networks," *Journal of Sound and Vibration*, vol. 388, pp. 154–170, 2017.

[36] Y. Kim, J. S. Park, B. K. Oh et al., "Practical wireless safety monitoring system of long-span girders subjected to construction loading a building under construction," *Measurement*, vol. 146, pp. 524–536, 2019.

[37] D. Liu, Z. Tang, Y. Bao, and H. Li, "Machine-learning-based methods for output-only structural modal identification," *Structural Control and Health Monitoring*, vol. 28, no. 12, 2021a.

[38] N. J. Alex Graves, *Hybrid Speech Recognition With Deep Bidirectional*, LSTM University of Toronto Department of Computer Science 6 King's College Rd, Toronto, Canada, 2013.

[39] Y. Bengio, R. Ducharme, P. Vincent, and C. Jauvin, "A neural probabilistic language model," *Journal of Machine Learning Research*, vol. 3, no. 6, 2003.

[40] J. Devlin, M. W. Chang, K. Lee, and K. Toutanova, "BERT: pre-training of deep bidirectional transformers for language understanding," *Proceedings of naacL-HLT*, vol. 1, 2019.

[41] H. Kim and S. H. Sim, "Automated peak picking using region-based convolutional neural network for operational modal analysis," *Structural Control and Health Monitoring*, vol. 26, no. 11, p. e2436, 2019.

[42] R. Yang, S. K. Singh, M. Tavakkoli et al., "CNN-LSTM deep learning architecture for computer vision-based modal

frequency detection," *Mechanical Systems and Signal Processing*, vol. 144, Article ID 106885, 2020.

[43] V. Mugnaini, L. Zanotti Fragonara, and M. Civera, "A machine learning approach for automatic operational modal analysis," *Mechanical Systems and Signal Processing*, vol. 170, 2022.

[44] J. L. Liu, A. H. Yu, C. M. Chang, W. X. Ren, and J. Zhang, "A new physical parameter identification method for shear frame structures under limited inputs and outputs," *Advances in Structural Engineering*, vol. 24, no. 4, pp. 667–679, 2021.

[45] F. Magalhães, Á. Cunha, E. Caetano, and R. Brincker, "Damping estimation using free decays and ambient vibration tests," *Mechanical Systems and Signal Processing*, vol. 24, no. 5, pp. 1274–1290, 2010.

[46] K. Kim, D. K. Kim, J. Noh, and M. Kim, "Stable forecasting of environmental time series via long short term memory recurrent neural network," *IEEE Access*, vol. 6, pp. 75216–75228, 2018.

[47] F. Magalhães, A. Cunha, and E. Caetano, "Vibration based structural health monitoring of an arch bridge: from automated OMA to damage detection," *Mechanical Systems and Signal Processing*, vol. 28, pp. 212–228, 2012.

[48] M. D. A Hasan, Z. A. B. Ahmad, M. Salman Leong, and L. M. Hee, "Enhanced frequency domain decomposition algorithm: a review of a recent development for unbiased damping ratio estimates," *Journal of Vibroengineering*, vol. 20, no. 5, pp. 1919–1936, 2018.

[49] S. Hochreiter, "The vanishing gradient problem during learning recurrent neural nets and problem solutions," *International Journal of Uncertainty, Fuzziness and Knowledge-Based Systems*, vol. 06, no. 02, pp. 107–116, 1998.

[50] S. Hochreiter and J. Schmidhuber, "Long short-term memory," *Neural Computation*, vol. 9, no. 8, pp. 1735–1780, 1997.

[51] M. Schuster and K. K. Paliwal, "Bidirectional recurrent neural networks," *IEEE Transactions on Signal Processing*, vol. 45, no. 11, pp. 2673–2681, 1997.

[52] S. Tong, H. Gu, and K. Yu, "A comparative study of robustness of deep learning approaches for VAD," in *Proceedings of the IEEE International Conference on Acoustics, Speech and Signal Processing- Proceedings*, Rhodes Island, Greece, May 2016.

[53] W. Kim, A. Yoshida, Y. Tamura, and J. H. Yi, "Experimental study of aerodynamic damping of a twisted supertall building," *Journal of Wind Engineering and Industrial Aerodynamics*, vol. 176, pp. 1–12, 2018b.

[54] A. Bajrić, R. Brincker, and S. Thöns, "Evaluation of damping estimates in the presence of closely spaced modes using Operational Modal Analysis techniques," in *Proceedings of the 6th International Operational Modal Analysis Conference*, Gijon, Spain, July 2015.

[55] S. Hochreiter and J. Schmidhuber, "Long short-term memory," *Neural Computation*, vol. 9, no. 8, pp. 1735–1780, 1997b.

[56] D. P. Kingma and J. L. Ba, *Adam: A Method for Stochastic Optimization*, 3rd International Conference on Learning Representations, San Diego, CA, USA, 2015.

[57] S. Ruder, "An overview of gradient descent optimization algorithms," 2016, https://arxiv.org/abs/1609.04747.

[58] M. Stuart, D. C. Hoaglin, F. Mosteller, and J. W. Tukey, "Understanding robust and exploratory data analysis," *The Statistician*, vol. 33, no. 3, p. 320, 1984.